©IDOSR PUBLICATIONS
INTERNATIONAL DIGITAL ORGANIZATION FOR SCIENTIFIC RESEARCH ISSN: 2550-794x
IDOSR JOURNAL OF SCIENTIFIC RESEARCH 1(1): 1-27, 2016.

Interpretation of High Resolution Aeromagnetic Data of Chibok and Damboa in North Eastern Nigeria Using Spectral Analysis Method for Hydrocarbon Potential

[1]Bala G.A, [2]Wante H.P and [3]Ngaram S.M

[1, 3]Department of Physics, Federal University Gashua, Yobe State, Nigeria.

[2]Department of Science Laboratory Technology (Physics Unit), Federal Polytechnic Mubi, Adamawa State, Nigeria.

Corresponding Author: gabpoonen@yahoo.com

ABSTRACT

High resolution Aeromagnetic data of Chibok and Damboa area (sheet 112 and 134 respectively), north eastern Nigeria, has been interpreted by applying spectral analysis technique in order to appraise the hydrocarbon accumulation potential of the area. The regional field was separated with a first order polynomial using Winglink software. The Total Magnetic Intensity Map (TMI) was subdivided into 18 spectral blocks allowing probe of 12.5km by 12.5km area for 15 minutes by 15 minutes windowing using Surfer 10 software. Two prominent magnetic depth source layers were identified. The deeper source depth values obtained ranges from 1.592km to 4.093kmwith an average depth of 2.390km as the magnetic basement depth while for the shallower source the depth values ranges from 0.403km to 0.795km with an average of 0.567km. The shallower depth source could attribute to the volcanic rocks that intruded the sedimentary formation and could possibly responsible for the mineralization found in parts of the study area. The significance of the magnetic depth values indicate that the sedimentary layer of the Albian age, Coniacian-Turonian age, and Turonian-Senonian age is thick enough to generate hydrocarbon. The temperatures at these depths range from 81.65°C to 169.16°C for the deeper sources and from 31.12°C to 32.82°C for the shallow sources. The temperature at the deep depth also satisfies a great condition for hydrocarbon generation/accumulation.

Keywords: Aeromagnetic, Spectral, Resolution, Depth, Geology and Exploration.

INTRODUCTION

Magnetic surveying investigates the sub-surface based on variations in the earth's magnetic field that result from the magnetic properties of the underlying rocks. Airborne geophysical surveying is a process of measuring the variation of several key physical or geochemical parameters of the earth. The most important parameters measured are conductivity, magnetic susceptibility, rock density, radioactive element concentration, and reflectance spectra. Any change in the Earth's near surface that causes a measurable change in these parameters, presents a potential application for airborne geophysics. Airborne geophysics has always been at the forefront of technological developments and innovation. Modern exploration systems can measure minute changes in the geophysical properties of the earth with high sensitivity instruments and survey platforms. Exploration projects utilize GPS navigation and timing, laser and radar altimeters, satellite communications and innovative data processing techniques. The main use of any aeromagnetic data and their derivative maps in mineral prospecting is to make geological deduction from them [1]. And from the range of magnetic intensity values of these data, information on subsurface lithology, trend and geological structures can be obtained. Airborne geophysical surveys are used for oil and mineral exploration, engineering projects, geothermal mapping, land management, and for mapping exposed bedrock, geological structures (such as basements, faults, dikes, sills, kimberlites), sub-surface conductors, paleochannels, minerals deposits and salinity.

In geophysics, a magnetic anomaly is a local variation in the Earth's magnetic field resulting from variations in the chemistry or magnetism of the rocks. Mapping of variations over area is valuable in detecting structures obscured by overlying materials. Magnetic anomaly maps provide insight into the sub-surface structure and composition of the earth's crust. Anomalies trending parallel to the isochron (lines of equal age) in the ocean reveal the temporal evolution of oceanic crust.

Since the release of aeromagnetic data in Nigeria by the Nigerian Geological Survey Agency (NGSA), there has been an upsurge of interest in the quantitative and qualitative interpretations of aeromagnetic data. Most recently, the chad basin in the North east has been Nigeria Government target to explore hydrocarbon. Interpretation of data from the region has been intensified.Interpretation of aeromagnetic data is aimed at mapping the subsurface regional structures (intrusive bodies, contacts, faults, basement rocks and mineralization). This could be performed both qualitatively and quantitatively. Qualitative interpretation involves the description of the survey in terms of the types of likely geological formation and structures that give rise to the evident anomalies. Typically, some geological information is available from outcrop evidence within the survey the survey area and very often the role of geophysical data is to extend this geological knowledge into areas where there is no outcrop information (that is extrapolation from known to unknown) or to extend mapped units into depths dimensions (that is to help add the third dimension to the mapped geology) [2].

Several quantitative methods of interpretation of aeromagnetic data that could be employed include: spectral analysis, analytical signal method, the Euler-3D methods, forward and inverse modelling method and graphical interpretation methods. Quantitative interpretation involves making numerical estimates of the depth dimensions of the sources of anomalies and this often takes the form of modelling of sources which could, in theory, replicate the anomalies calculated in order to see whether the earth-model is consistent with that has been observed, that is, given a model that is a suitable physical approximation to the unknown geology, the theoretical anomaly of the model is calculated (forward modelling) and compared with the observed anomaly. The beginning of stages of magnetic data interpretations generally involve the application of mathematical filters such as the separation of regional field from the residual field, first and second vertical derivative filters etc to the observed data. The specific goals of these filters vary depending on the situation. The general purpose is to enhance anomalies of interest and/or gain some preliminary information on the source location or magnetization.

Location of the Area

The study areas (Fig. 1) are in Borno state (combined Chibok and Damboa sheet), North eastern Nigeria in the southern part of Chad Basin. The study area is bounded by latitudes 11° 13 - 12° 30'N and longitudes 13° 00'- 14°00' E. Part of the study area is located within the sedimentary terrain of the Chad Basin. The geology of Nigeria is made up of three major litho-petrological components, namely; the basement complex, younger granite and the sedimentary basins. The Chad Basin is the largest intracratonic Basin in Africa [3], covering an area of about 233,000km^2. It straddles five countries namely; Nigeria, Chad republic, Niger republic, Cameroon and Central African Republic [4]. Its western margin is marked by the water shade between the river Niger and river Chad drainage systems, and approximately one-tenth of the surface area of the Chad Basin is in the North-East Nigeria, bounded to the east by the Massif (Mandara Mountains) and in the south by the Benue Trough and Biu Plateau [5]. The origin of the Chad Basin is associated with the separation of the African and South American continents in the early Cretaceous [5, 6, 7 and 8] and from the structural styles, there is a strong indication that the evolution of the Chad.

With the vision of ascertaining the basement morphology and hydrocarbon bearing potential of the study area, which could probably add to the economy of the nation thus reducing the dependence of the ever depleting Niger delta basin, the present study was undertaken.

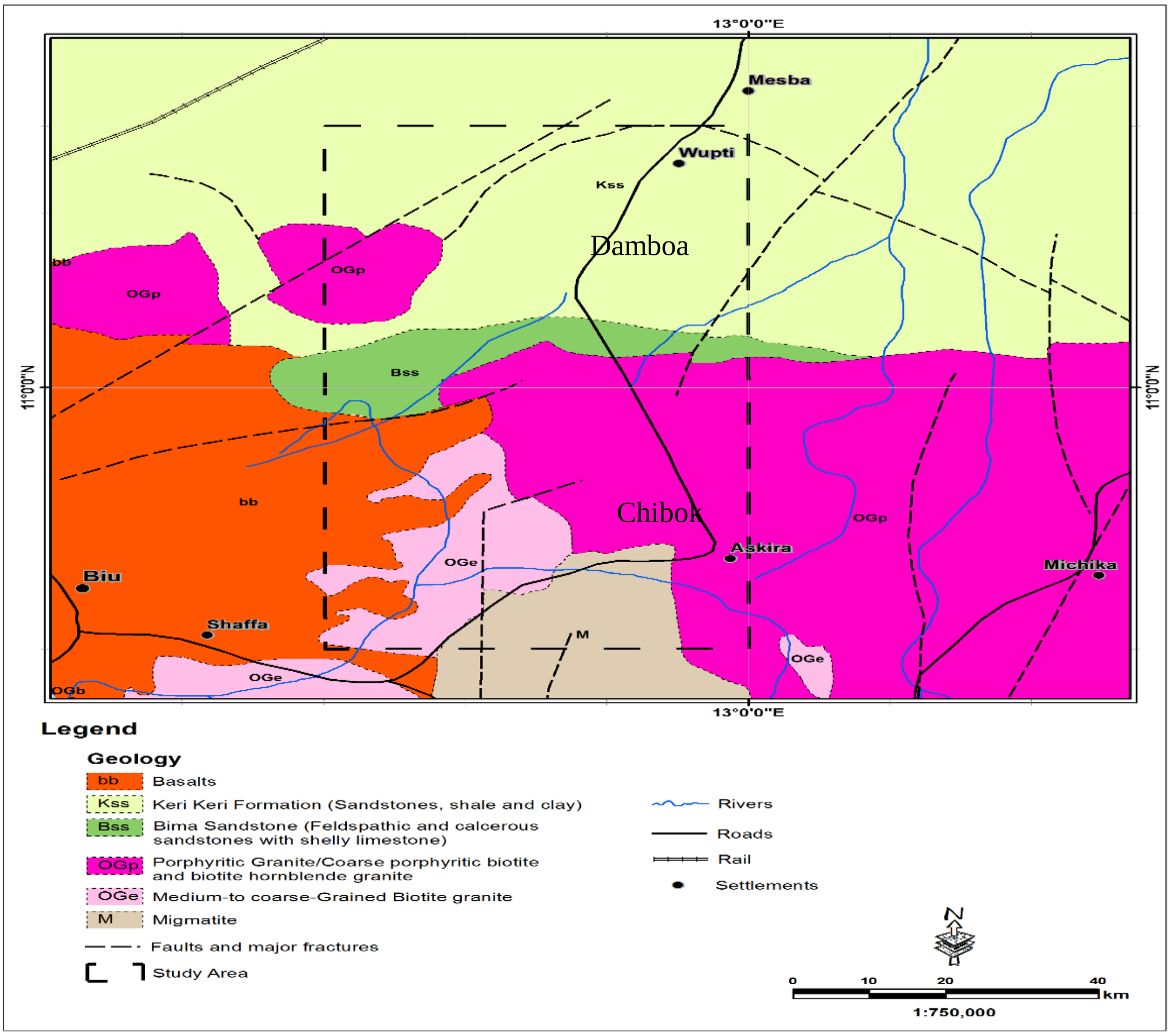

Fig.1:Geological map of the study area.

MATERIALS AND METHODS

Two sheets were assembled for this study (112,134) with each square block representing a map in a scale of 1:100,000. Each square block is about 55 by 55 km^2 covering an area of 3025 km^2 hence the total area studied was about 6050 km^2. The new high resolution airborne survey carried out for the Nigerian Geological Survey Agency by Fugro airborne services in 2009 used for this study was flown at 500m line spacing and

80m terrain clearance using various survey parameters, software's and errors corrected during surveys.

Theoretical Background on Spectral Analysis.

The Discrete Fourier Transform is the mathematical tool for spectral analysis and applied to regularly spaced data such as the aeromagnetic data. The Fourier Transform represented mathematically in Onwuemesi, (1997) [9] as:

$$Y_{i(x)} = \sum_{n=1}^{\infty} \left(a_n \cos\frac{2n\pi x}{L} + b_n \sin\frac{2n\pi x}{L} \right) \qquad 1.0$$

Where $Y_{i(x)}$ is reading of the Fourier Transform at x_i position, L is length of the cross-section of the anomaly, n is harmonic number of the partial wave number of data points, a_n is real part of the amplitude spectrum and b_n is imaginary part of the amplitude spectrum for $i = 0,1,2,3, \ldots\ldots n.$

It has become a familiar concept to interpret aeromagnetic data with one or two dimensional spectral analysis consisting of various frequencies which characterize the anomalies. The application of the power spectrum method to potential field data was proposed by Bhattacharyya (1966) [10]; and the determination of the anomalous body depth was given by Spector and Grant, (1970) [11]. This method has been used extensively by many researchers like Mishra and Naidu (1974) [12]; Ofoegbu and Onuoha (1991). [13] It is based on the principle that a magnetic field measured at the surface can be considered the integrals of magnetic signatures from all depths. The power spectrum (obtained through Fourier transform) of the surface field can be used to identify average depths of source ensembles. In its complex form, the two dimensional Fourier transform pair may be written as in equations $1.1\ and\ 1.2$ [14].

$$G(u,v) = \iint_{-\infty}^{\infty} g(u,v)\, e^{i(Ux-Vy)}\, dx\, dy. \qquad 1.1$$

$$G(x,y) = \frac{1}{4\pi^2} \iint_{-\infty}^{\infty} g(u,v) e^{i(Ux-Vy)}\, du\, dv. \qquad 1.2$$

Where u and v are the angular frequencies in x and y directions respectively. $G(u,v)$when broken up into its real and imaginary parts is given as in equation 1.3:

$$G(u,v) = P(u,v) + iQ(u,v) \qquad 1.3$$

The energy spectrum is given by equation 1.4 as

$$E(u,v) = [G(u,v)]^2 = (P^2 + Q^2) \qquad 1.4$$

Expression for the energy spectrum in polar form follows that [11];

If $r^2 = (u^2 + v^2)$ and $\theta = arctan(^u/_v)$ 1.5

The energy spectrum E(r, θ) could be given by;

$\langle E(r,\theta)\rangle = 4\pi^2 M^2 R_G^2 \langle e^{-2hr}\rangle \langle (1-e^{-tr})^2\rangle \langle S^2(r,\theta)\rangle \langle R_p^2(\theta)\rangle$,1.6

Where $\langle E(r,\theta)\rangle$ indicates the expected value, $r^2 = (u^2 + v^2)$ is the magnitude of the frequency vector and $\theta = arctan(^u/_v)$ is the direction of the frequency vector;

$M$is magnitude of the moment/unit depth, h is depth to the top of the prism,t is thickness to the top of the prism,S is factor for the horizontal size of the prism, R_p is the factor for magnetization of the prism and $R_G$is the factor for geomagnetic field direction.

The ensemble average depth h, enters only into the factor

$$\{e^{-2hr}\} = \frac{e^{2hr}\sinh(2r\Delta h)}{4r\Delta h} \qquad 1.7$$

The energy spectrum will then consist of two parts; the first spectrum which relates to the deeper source is relatively strong at the low frequencies and decays rapidly. The second spectrum which varies from the shallower ensembles of sources dominates the high frequency end of the spectrum. In general case, the radial spectrum may be conveniently approximated by straight line segments, the slopes of which relate to depths of the possible layers [15, 16, 17, 18 and 19].

The spectrum is to be extracted from the residual value of total magnetic field intensity values which are used to obtain the two dimensional Fourier transformation $T(x,y)$ consisting of $m$rows and $n$columns in the $x-y$ plane. The evaluation is done using an algorithm that is a two dimensional extension of the Fast Fourier Transformation [20]. Next the frequency intervals are subdivided into sub-intervals, which lie within one unit of frequency range. The average spectrum of the partial waves falling within this frequency range is calculated and the resulting values constitute the radial spectrum of the magnetic anomalies [21, 22, 23 and 24].

Conclusively, we plot the logarithm of energy values versus frequency on a linear scale and locate the linear segments. Each linear segment is due to anomalies caused by bodies accruing within a particular depth. If $Z$is the mean depth of layer, the depth factor for this ensemble of anomalies is $exp(-2zk)$.

The mean depth of burial of the ensemble is thus determined using [25, 26, 27].

$$Z = -m/2\pi \qquad 1.8$$

Where m is the slope of the best fitting straight line.

DATA ANALYSIS AND RESULTS

The following operations were performed on the acquired digitized aeromagnetic data leading to the quantitative determination of depth to magnetic sources.

1. Regional-Residual Separation.

The regional field was removed from the total magnetic intensity data (Fig. 2a and 2b) to obtain the residual data with a first order polynomial using Winglink program. The residual data was subdivided into 18 spectral cells allowing spectral probe of 12.5km by 12.5km area for 15 minutes by 15 minutes windowing.

2. Division into Spectral Cell and Windowing.

For the purpose of easier handling of the large data involved the two residual block of the study area was subdivided into 18 spectral cells (Fig. 4) 12.5km by 12km in order to accommodate longer wavelength so that depth to about 12km could be investigated. Each signal was then windowed 15 minutes by minutes.

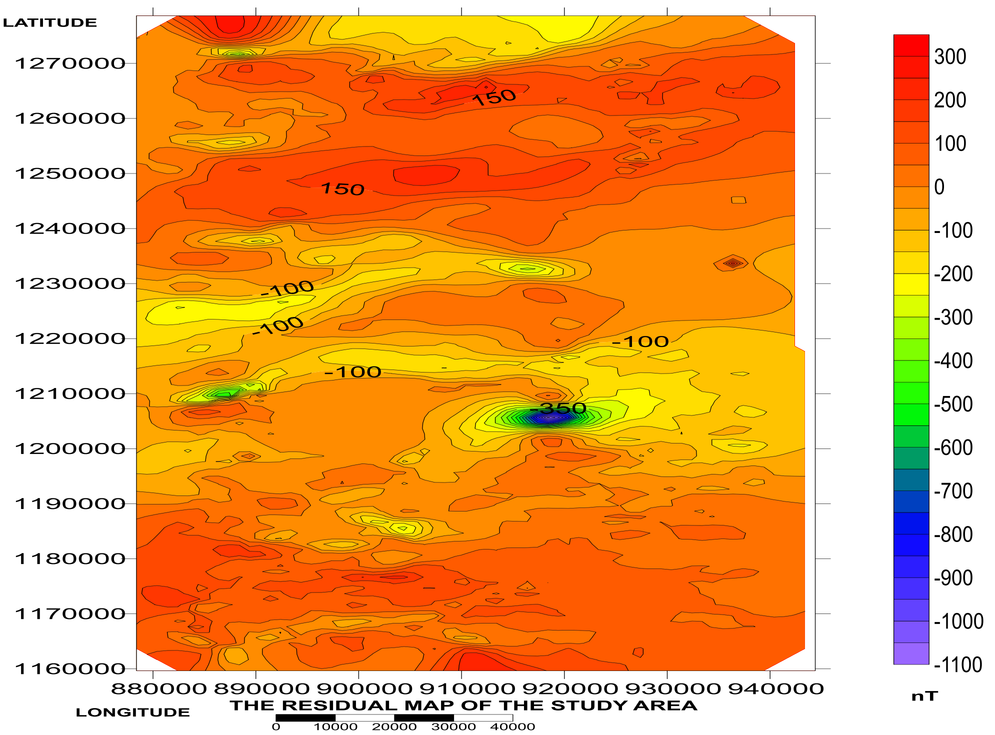

Fig.2 (a).The residual anomaly map.

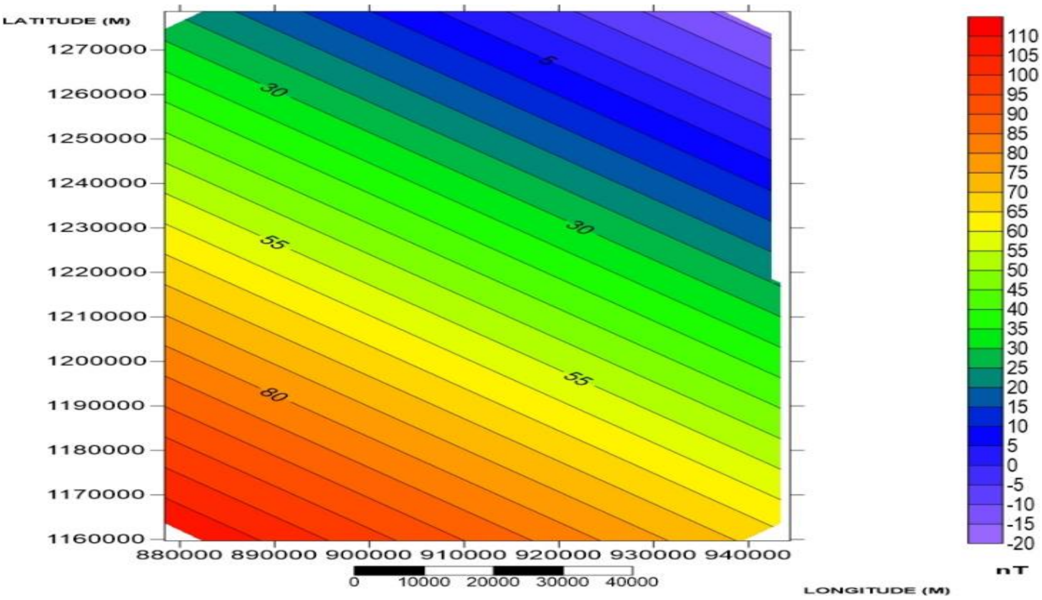

Fig. 2(b).The regional anomaly map.

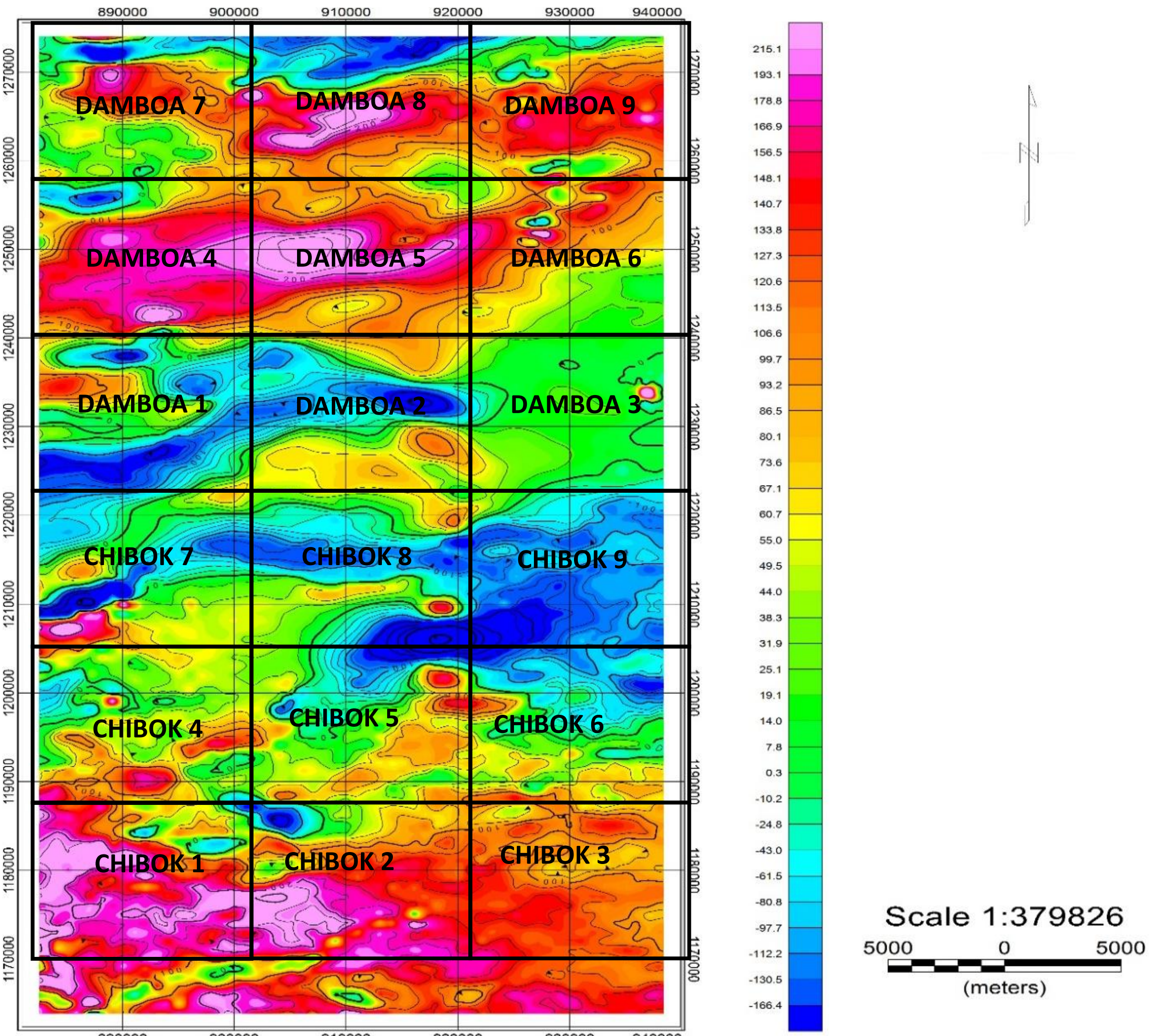

Fig. 3 The TMI showing the 18 spectral block.

1. Generation of Radial Energy Spectrum.

Digital signal processing software program employing the fast Fourier transform technique was used to transform the residual magnetic data into the radial energy spectrum for each block. The average radial power spectrum was calculated and displayed in a semi-log figure of amplitude versus frequency.

2. Plots of Log of Energy and the Frequency.

Spector and grant, (1970) [11] have shown that the log spectrum of the source have a linear gradient whose magnitude is dependent upon the depth of the source. Graphs of logarithm of the spectral energy against the frequencies for the 18 spectral cells was plotted and shown on Fig. 4.

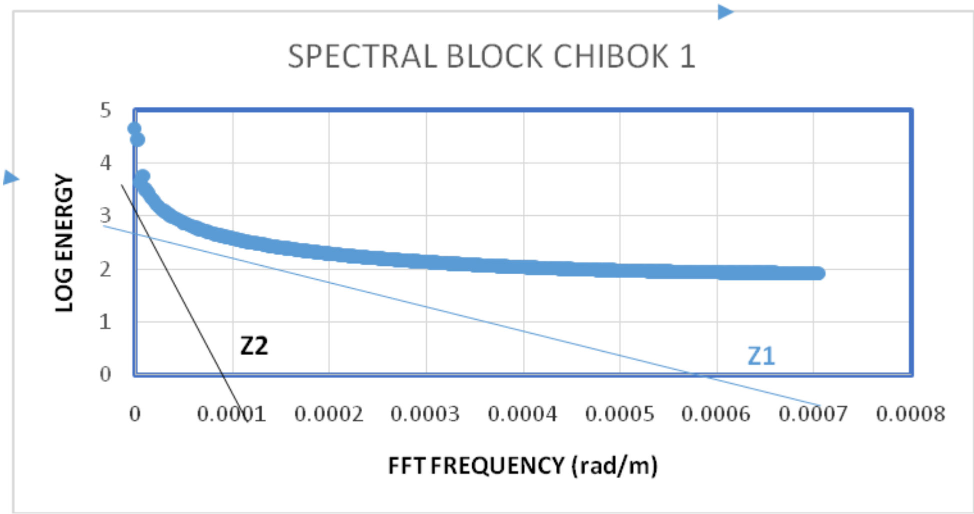

(a)

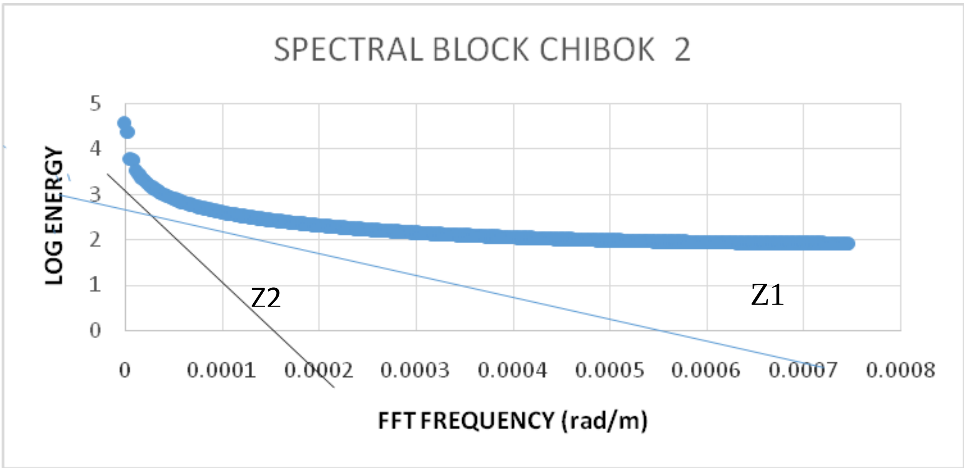

(b)

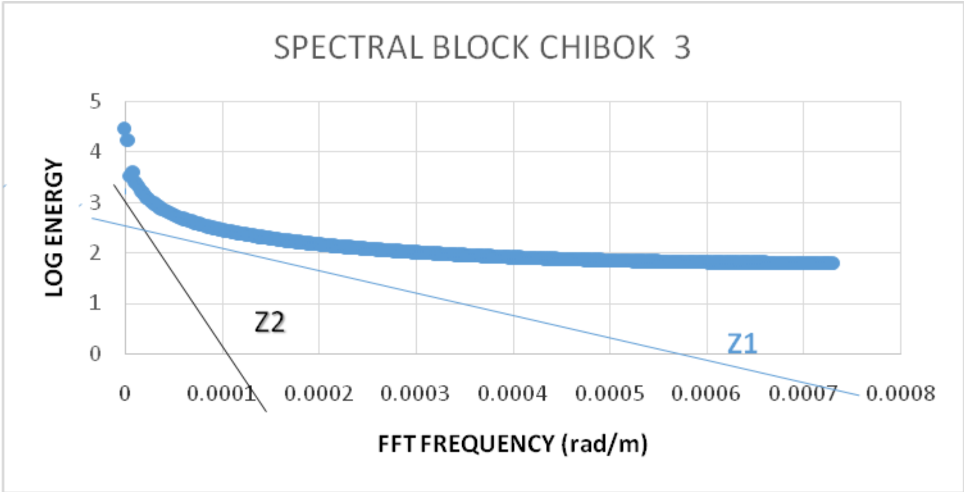
SPECTRAL BLOCK CHIBOK 3
LOG ENERGY
FFT FREQUENCY (rad/m)
Z2
Z1
0
1
2
3
4
5
0.0001
0.0002
0.0003
0.0004
0.0005
0.0006
0.0007
0.0008

(c)

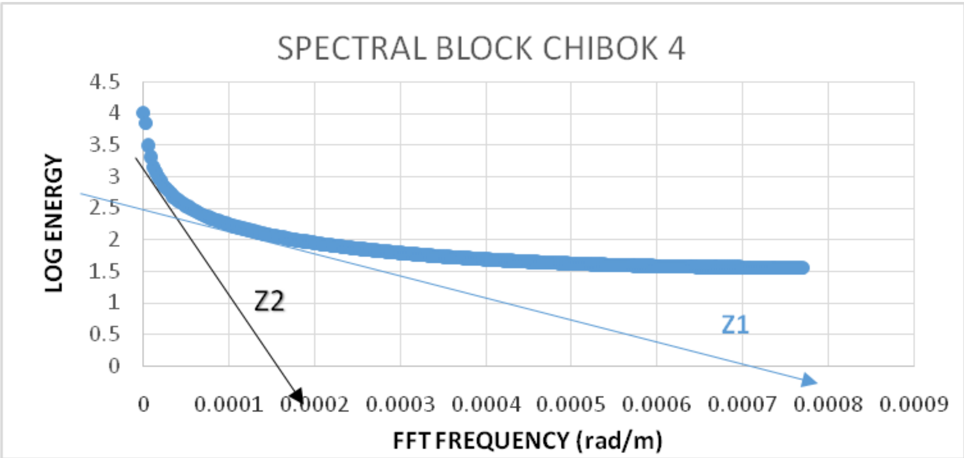
SPECTRAL BLOCK CHIBOK 4
LOG ENERGY
FFT FREQUENCY (rad/m)
Z2
Z1
0
0.5
1
1.5
2
2.5
3
3.5
4
4.5
0.0001
0.0002
0.0003
0.0004
0.0005
0.0006
0.0007
0.0008
0.0009

(d)

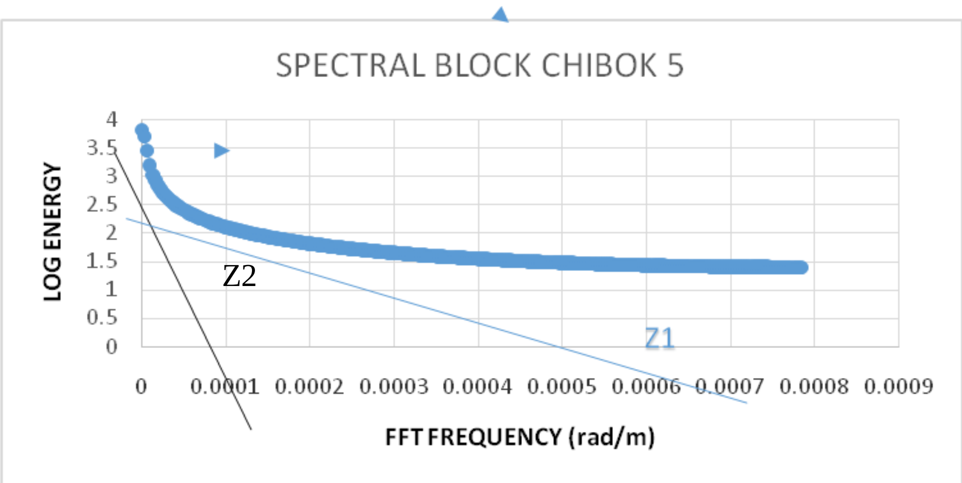
SPECTRAL BLOCK CHIBOK 5
LOG ENERGY
FFT FREQUENCY (rad/m)
Z2
Z1
0
0.5
1
1.5
2
2.5
3
3.5
4
0.0001
0.0002
0.0003
0.0004
0.0005
0.0006
0.0007
0.0008
0.0009

(e)

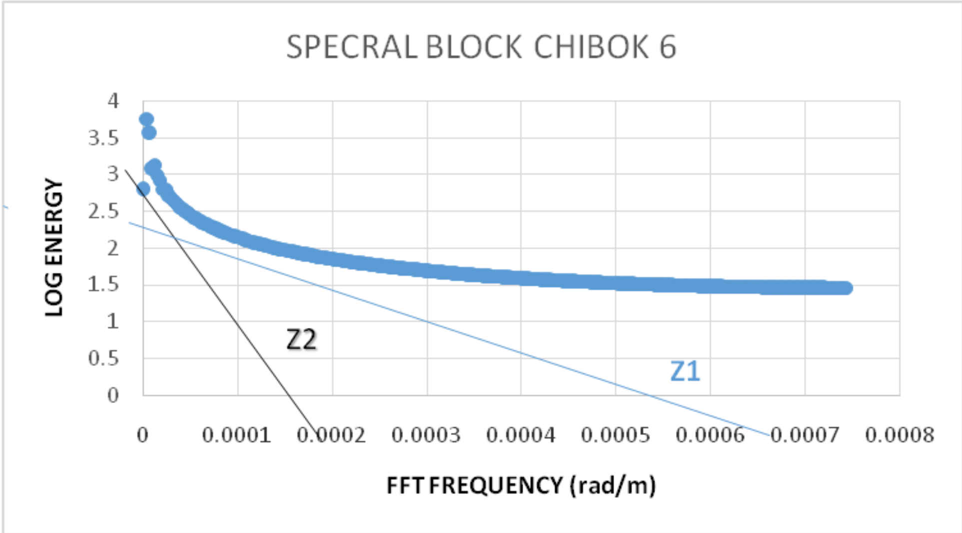
SPECRAL BLOCK CHIBOK 6
LOG ENERGY
FFT FREQUENCY (rad/m)
Z2
Z1
0
0.5
1
1.5
2
2.5
3
3.5
4
0
0.0001
0.0002
0.0003
0.0004
0.0005
0.0006
0.0007
0.0008

(f)

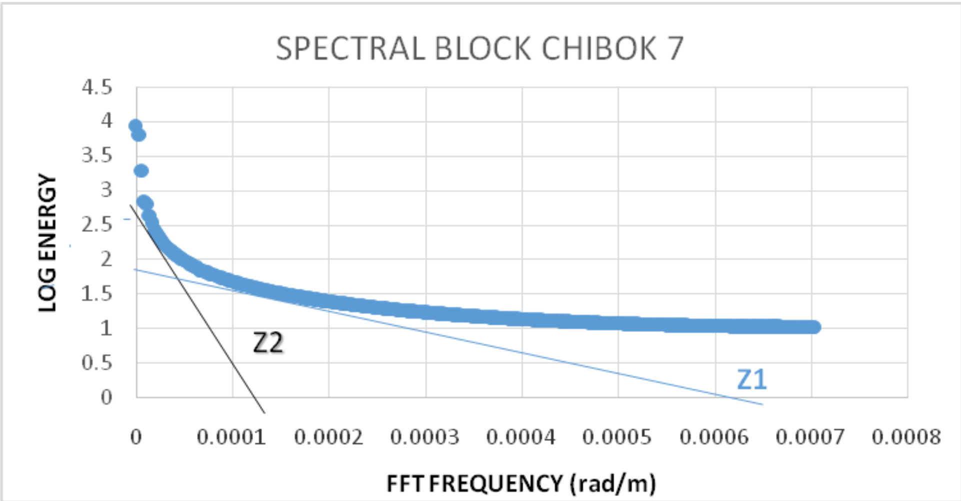
SPECTRAL BLOCK CHIBOK 7
LOG ENERGY
FFT FREQUENCY (rad/m)
Z2
Z1
0
0.5
1
1.5
2
2.5
3
3.5
4
4.5
0
0.0001
0.0002
0.0003
0.0004
0.0005
0.0006
0.0007
0.0008

(g)

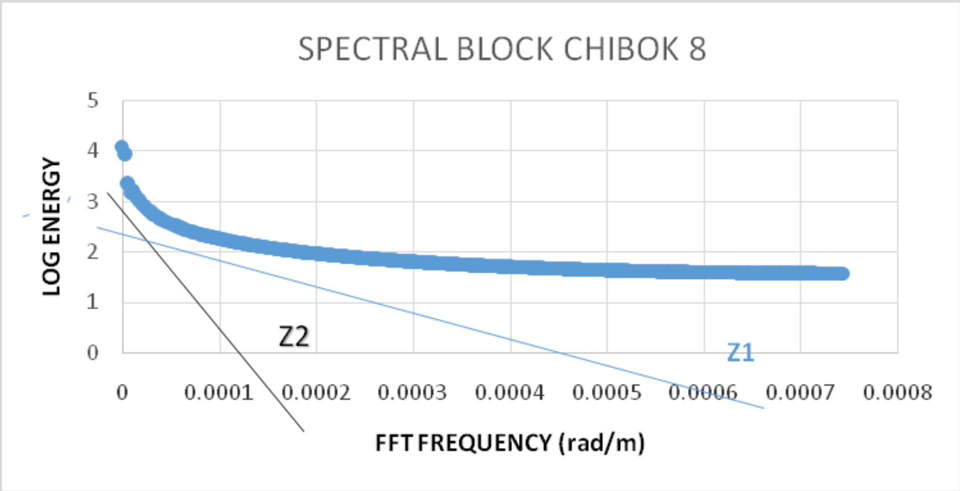
SPECTRAL BLOCK CHIBOK 8
LOG ENERGY
5
4
3
2
1
0
Z2
Z1
0
0.0001
0.0002
0.0003
0.0004
0.0005
0.0006
0.0007
0.0008
FFT FREQUENCY (rad/m)

(h)

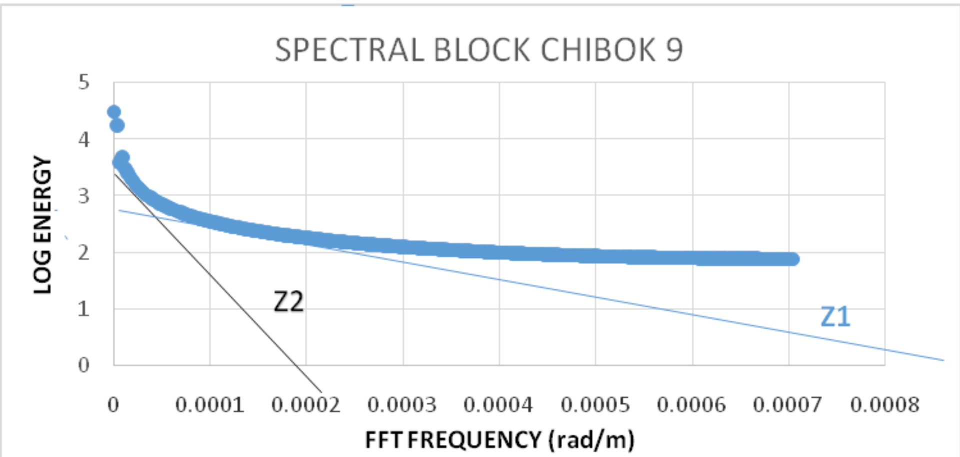
SPECTRAL BLOCK CHIBOK 9
LOG ENERGY
5
4
3
2
1
0
Z2
Z1
0
0.0001
0.0002
0.0003
0.0004
0.0005
0.0006
0.0007
0.0008
FFT FREQUENCY (rad/m)

(i)

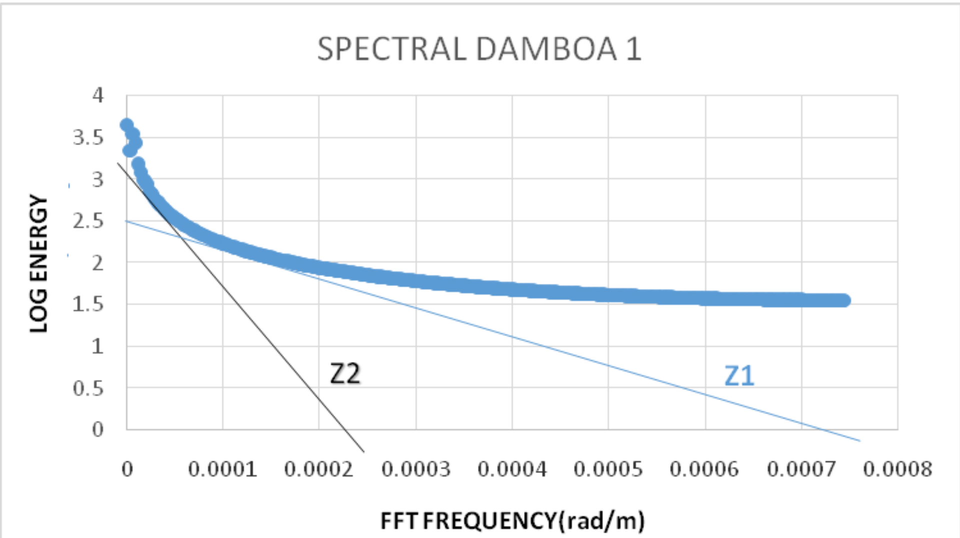
SPECTRAL DAMBOA 1
LOG ENERGY
4
3.5
3
2.5
2
1.5
1
0.5
0
Z2
Z1
0
0.0001
0.0002
0.0003
0.0004
0.0005
0.0006
0.0007
0.0008
FFT FREQUENCY(rad/m)

(j)

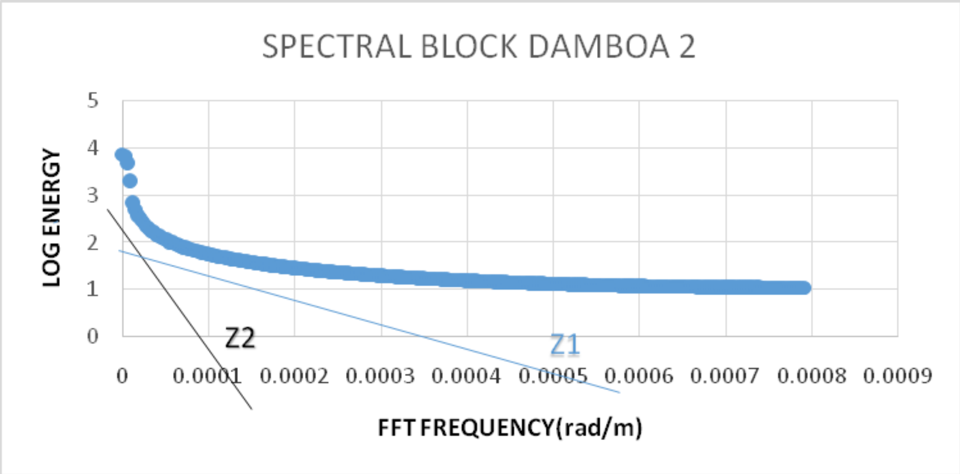
SPECTRAL BLOCK DAMBOA 2
LOG ENERGY
5
4
3
2
1
0
Z2
Z1
0
0.0001
0.0002
0.0003
0.0004
0.0005
0.0006
0.0007
0.0008
0.0009
FFT FREQUENCY(rad/m)

(k)

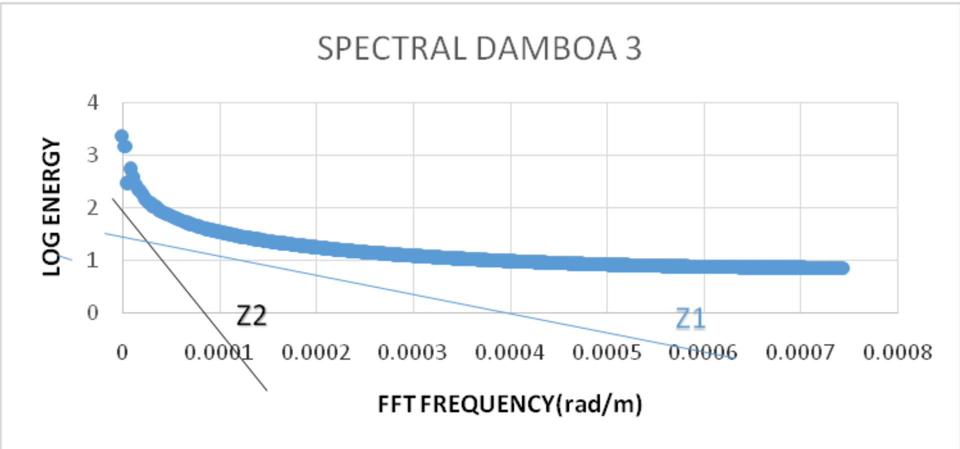
SPECTRAL DAMBOA 3
LOG ENERGY
4
3
2
1
0
Z2
Z1
0
0.0001
0.0002
0.0003
0.0004
0.0005
0.0006
0.0007
0.0008
FFT FREQUENCY(rad/m)

(l)

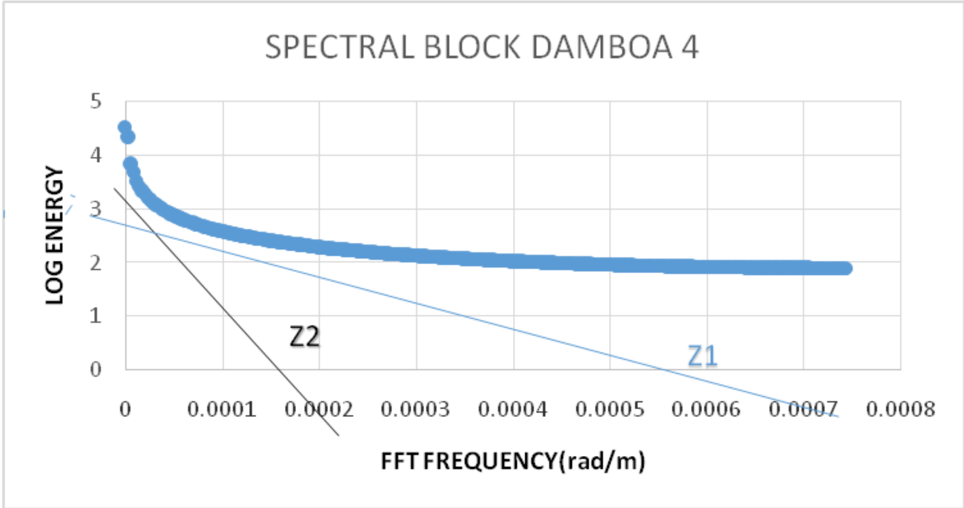

SPECTRAL BLOCK DAMBOA 4
LOG ENERGY
FFT FREQUENCY(rad/m)
Z2
Z1
0
1
2
3
4
5
0
0.0001
0.0002
0.0003
0.0004
0.0005
0.0006
0.0007
0.0008

(m)

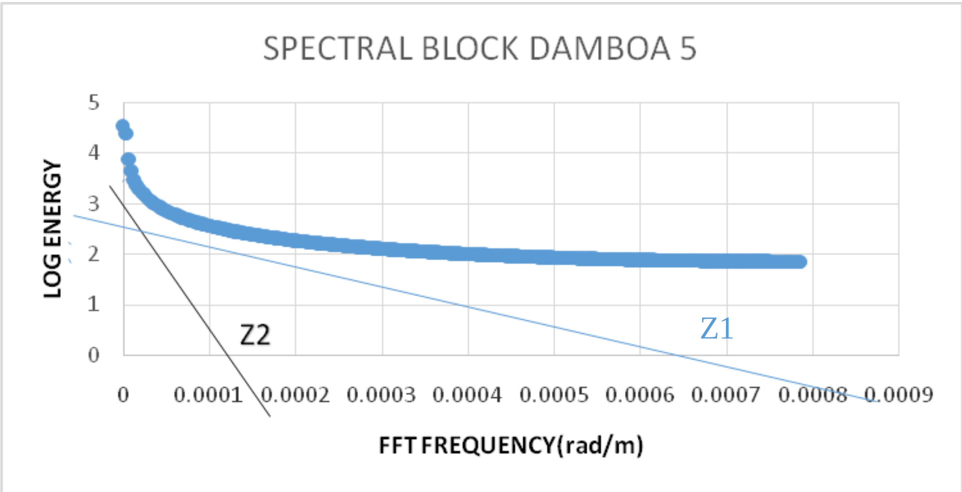

SPECTRAL BLOCK DAMBOA 5
LOG ENERGY
FFT FREQUENCY(rad/m)
Z2
Z1
0
1
2
3
4
5
0
0.0001
0.0002
0.0003
0.0004
0.0005
0.0006
0.0007
0.0008
0.0009

(n)

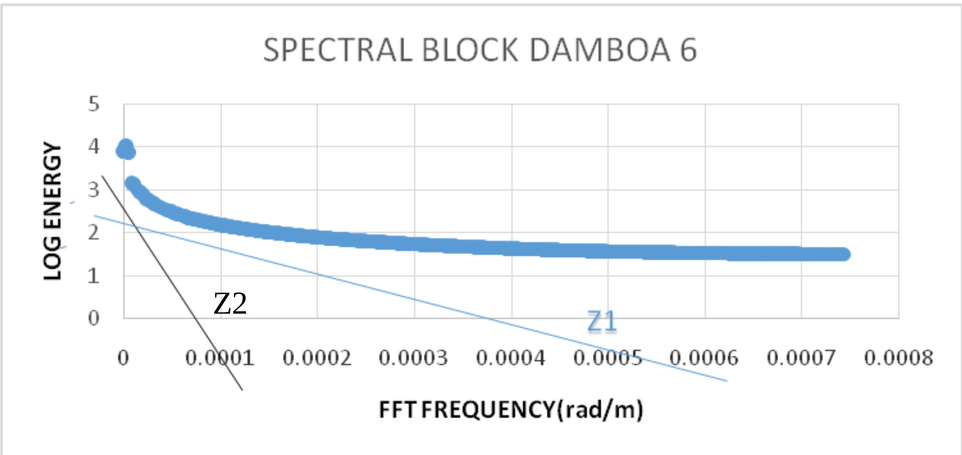

SPECTRAL BLOCK DAMBOA 6
LOG ENERGY
FFT FREQUENCY(rad/m)
Z2
Z1
0
1
2
3
4
5
0
0.0001
0.0002
0.0003
0.0004
0.0005
0.0006
0.0007
0.0008

(o)

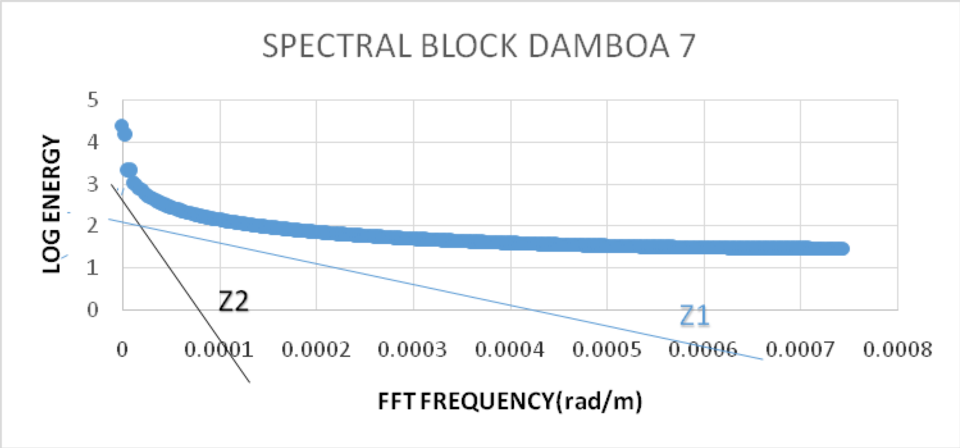
SPECTRAL BLOCK DAMBOA 7
LOG ENERGY
5
4
3
2
1
0
Z2
Z1
0
0.0001
0.0002
0.0003
0.0004
0.0005
0.0006
0.0007
0.0008
FFT FREQUENCY(rad/m)

(p)

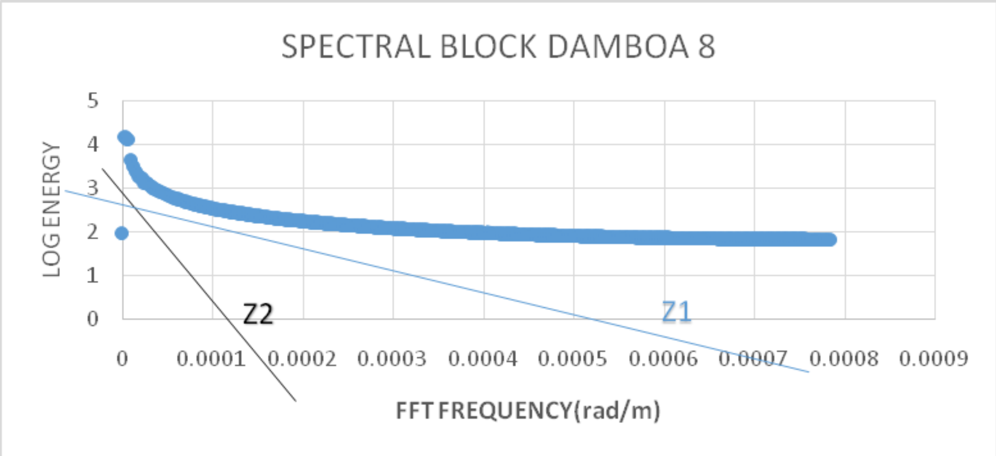
SPECTRAL BLOCK DAMBOA 8
LOG ENERGY
5
4
3
2
1
0
Z2
Z1
0
0.0001
0.0002
0.0003
0.0004
0.0005
0.0006
0.0007
0.0008
0.0009
FFT FREQUENCY(rad/m)

(q)

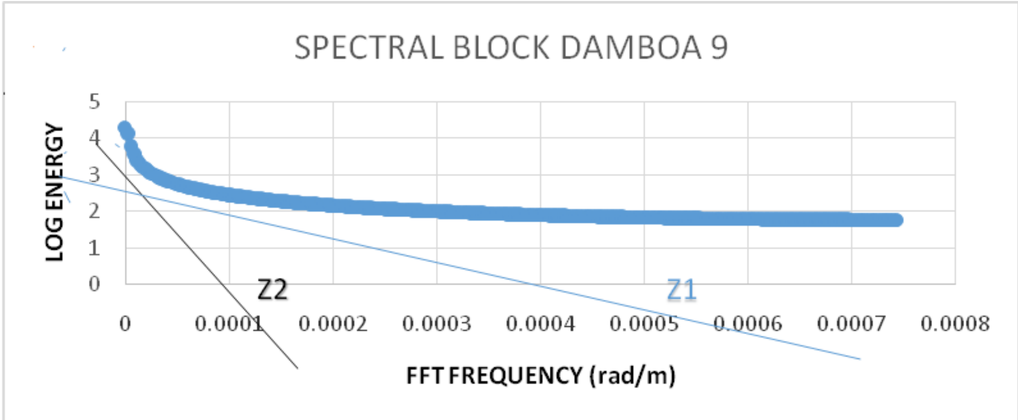
SPECTRAL BLOCK DAMBOA 9
LOG ENERGY
5
4
3
2
1
0
Z2
Z1
0
0.0001
0.0002
0.0003
0.0004
0.0005
0.0006
0.0007
0.0008
FFT FREQUENCY (rad/m)

(r)

Fig. 4 (a-r): Plot logarithm of the spectral energy against frequency**.**

For each cell two linear segments could be identified which implies that there are two magnetic source layers in the study area. Each linear segment group points are due to anomalies caused by bodies occurring within a particular depth range. The line segment in the higher frequency range is from the shallow sources and the lower harmonics are indicative of sources from deep-seated bodies.

3. Estimation of Depth to Magnetic Sources

The gradient m of each of the line segments were evaluated. And is given as;

$$m = \frac{\Delta \log E}{\Delta frequency} \qquad 1.11$$

The mean depth (z) of the burial ensemble was as;

$$z = -\frac{m}{2} \qquad 1.12$$

The coordinates and the two depth estimates $(z_1 and\, z_2)$ for each of the eighteen spectral blocks are given in table 1.

4. Estimation of Temperature at Depth

Heat is transferred through the upper layers mainly by conduction; only small part of the heat is transported by advection like volcanism and fluid circulations. The temperature distribution in the upper layers can be determined with information about the heat flow from the underlying convecting mantle, the distribution of radioactive elements, the surface temperature, and the thermal conductivity. All of these parameters can vary with time and location, commonly, the thermal conductivity is treated as a constant bulk property in other to derive the depth of water ice layers [28], to constrain the surface heat flow as function of time [28, 29] and to calculate the thermal evolution [30, 31]. This simplified view neglects that the thermal conductivity is a highly variable parameter that depends on the temperature.

Geologists often refer to the temperature range in which oil forms as oil window, below the minimum temperature, the organic matters remain trapped in the form of Kerogen and above the maximum temperature the oil is converted to natural gas through the process of thermal cracking. Usually, the oil window is often found in the 60-120°C interval with approximate depth of 2-4km, this values falls within the range of the thickness to sediment calculated with spectral analysis [32, 33, 34 and 35].

$$T_z = mz + T_o \qquad 1.13$$

Where

T_z= temperature at depth in °C at depth (z); m = geothermal gradient; z= depth of interestandT_o= surface temperature.

It was further assumed that the surface temperature was 30°C, while the average geothermal gradient in the study area was given by. Nwankwo and Ekine, (2009) as 3.4°C/100m. Equation 1.13 will be used to compute the temperature at both the deep and the shallow depth.

The deep anomaly source depth averaging 2.390km deep represent the magnetic basement surface of the study area while the other depth averaging 0.567km represents the shallow source.

Magnetic Basement Surface Plot

Making use of z_2 data, the surface plot of the magnetic basement depth depicting its undulating nature was plotted with surfer32 software and shown on Fig. 5. (a&b)

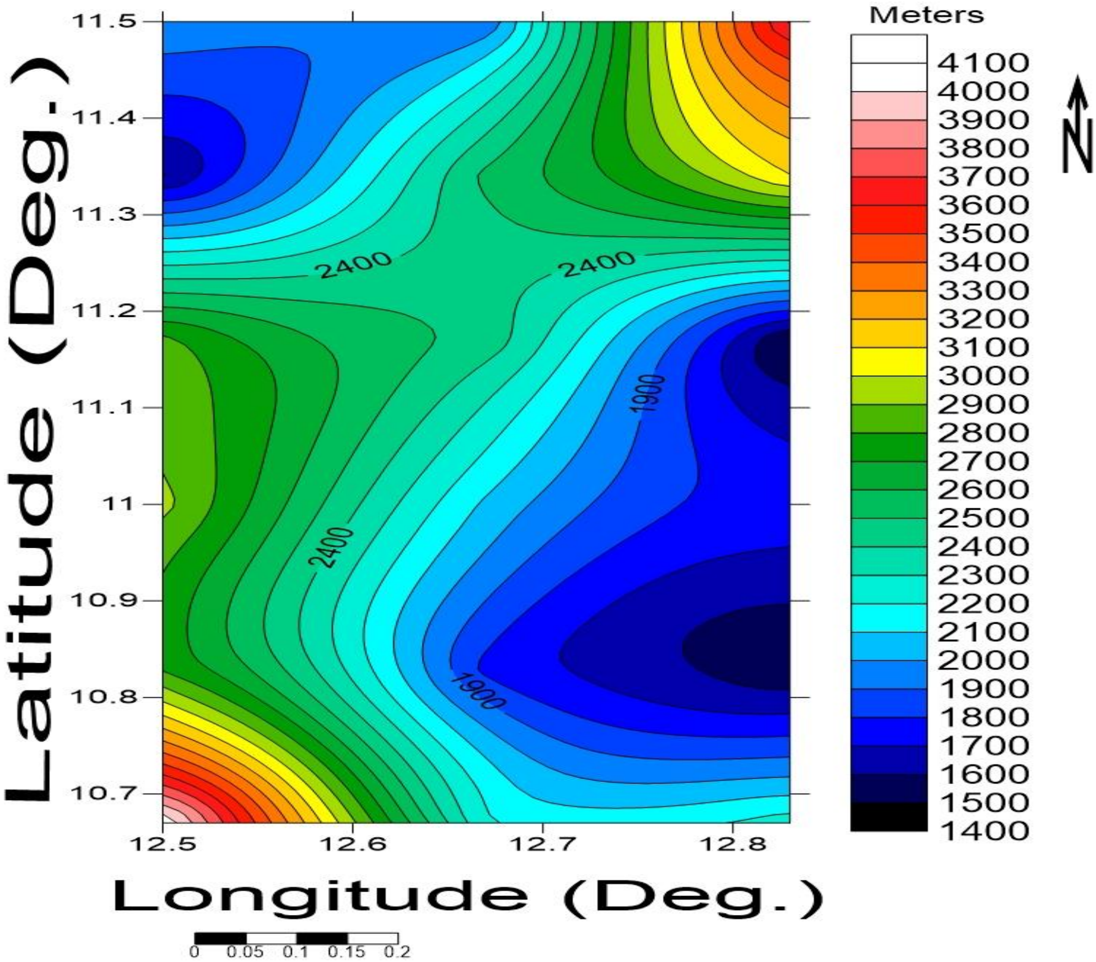

Fig. 5(a): 2-D contour plot of the magnetic surface. (Contour interval of 100km)

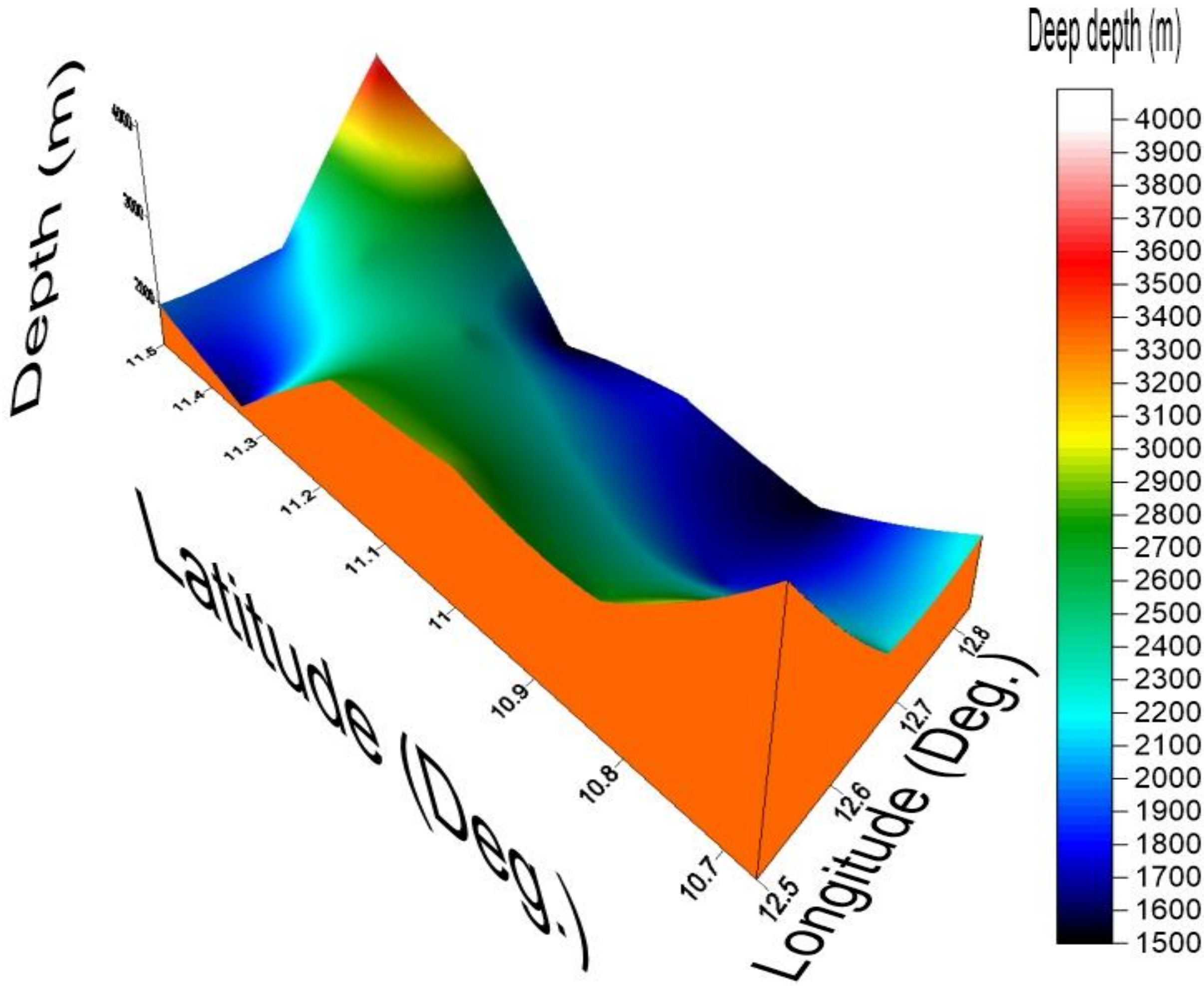

Fig. 5 (b): 3-D model of the magnetic basement surface of the study area.

DISCUSSION

Spectral analysis of the high resolution aeromagnetic data of Chibok and Damboa areas in the chad basin has revealed two main magnetic anomaly sources depth as shown in Fig 5 (a&b). These are the deep magnetic anomaly sources and the shallow magnetic anomaly sources. The deep sources anomalies vary between 1.485km and 4.093km with an average depth of 2.390km and this represents the magnetic the magnetic basement depth. The shallow anomaly source varies from 0.361km to 0.844km with an average of 0.567km and this may be regarded as the magnetic intrusions into the sediment. These depth results agree with some depth results obtained by other research works done in the Chad basin [8, 17, 19 and 29]. This represents the average thickness of the sedimentary formation that overlay the basement complex within the central portion of the study area. Four maps were produced from the result of the spectral analysis for visual interpretation; these are the depth to basement contour maps and the 3D construction of the subsurface for both the deep and the shallow depths, Fig. 4.9 (a, b) and Fig.4.10 (a, b) respectively. The revelation from this study of 2.390km magnetic basement depth is synonymous to depth of overburden sediment which has a very important significance as regards to the hydrocarbon generation potential of the area.

The temperatures at depth, ranges from 81.65°C to 169.16°C with an average value of 125.41°C for the deeper depth, while it ranges from 31.12°C to 32.82°C with an average value of 31.90°C for the shallow depth. The temperature range for the deep depth falls within what geologist call the oil window temperature (60-120°C), below which the organic matters remain trapped in the form of kerogen and above which the oil is converted to natural gas [15]. Wright et al., (1985) reported that when all other conditions for hydrocarbon accumulation are favourable, and the average temperature gradient of 1°C for 30m obtainable in oil rich Niger delta is applicable, then the minimum thickness of the sediment required for to achieve the threshold temperature of 115°C for the commencement of oil formation from marine organic remains would be 2.3km deep. Therefore, the calculated maximum depth of 4.093 from the study area is sufficient for oil to generate if other basic conditions are met.

CONCLUSION

Sedimentary basins are very important and should not be neglected for all natural resource exploration purposes. Hydrocarbon accumulation and its potentials is enhanced by the thickness of the sediments of the Basin, and also by the kind of geological structures existing within the basement that form traps for oil and gas. Maximumdepth/thickness obtained from modelling results (2268 m), spectral analysis (4093.1 m), SPI (5026.6 m) and Euler deconvolution (2106.6 to 4808.6 m) show thick sediment that is fairly sufficient for hydrocarbon accumulation which agrees with the work of Wright *et al.* (1985) that the minimum thickness of the sediment required for the commencement of oil formation from marine organic remains would be 2300 m (2.3 km).The results obtained from the use of the new high resolution data have shown some similarities with results obtained by some previous researchers who used old aeromagnetic data. However, results from the new data shows a better striking features owing to the high resolution nature of the 2009 data more than the 1970s data in terms of terrain clearance, line spacing and improvement of technology. The depth values estimated from the spectral analysis and the values of magnetic susceptibilities are indication that mineral prospecting should be intensified. This work will help to ascertain a better geophysical details of the southern part of the Chad-Basin, and further enhanced the full coverage of the whole basin in the exploration activity.

RECOMMENDATION

Full scale seismic reflection and well logging work in the study area are recommended to fully ascertain the presence of hydrocarbon accumulation. Gravity and land magnetic survey should also be carried out in the study area to confirm the results obtained in this work, most especially in terms of the minerals present.

REFERENCES

1. Dobrin, M.B. and Savit, C.H. (1988):Introduction to geophysical prospecting.
2. Reeves, C. (2005):Aeromagnetic surveys principles, practice and interpretation. Geosoft.

3. Matheis, G. (1986): Short review of the geology of the Chad Basin in Nigeria, in C. A. Kogbe (ed). Geology of Nigeria: Elizabeth publishing, surulere Nigeria. 289-294.

4. Obaje, N.G.J., Wehner, H., Hamza, H.andScheeder, G. (2004): New Geochemical data from the Nigerian sector of the Chad basin: Implication on hydrocarbon propectively. *Journal of African Earth Sciences*, 38(5):477-487.

5. Burke, K.C., (1976): Development of graben associated with the initial rupture of the Atlantic Ocean I.: Sedimentary basins of continental margins andcratons, Tectonophysics, (36) 93-112.

6. Fairhead, J.D., and Blinks, R., (1991): Differential opening of the central and south Atlantic Oceans and the opening of the West African rift-system. Tectonophysics, (1987):191-203.

7. Genik, G.J. (1993): Petroleum Geology of Cretaceous-Tertiary rift Basin in Niger, Chad and Central African Republic. American Association of petroleum geologist, Bull. 77(8):1405-1434.

8. Chukwunonso, O.C., Onwuemesi, A.G., Emmanuel. A.K., Chinwuko, A.I., Ikumbur, B.E. and Usman, A.O., (2012): Aeromagnetic Interpretation over Maiduguri and Environs of Southern Chad Basin, Nigeria. *Journal of Earth Sciences and Geotechnical Engineering*, 2(3):77-93.

9. Onwuemesi, A. (1997). One-dimensional spectral analysis of aeromagnetic anomalies and Curie depth isotherm in the Anambra basin of Nigeria.Journal of Geodynamics, 23(2):95-107.

10. Bhattacharyya, B.K. (1966). Continuous spectrum of the total magnetic field anomaly due to a rectangular prismatic body. Geophysics, 31:97-121.

11. Spector, A., Grant, F.S. (1970). Statistical models for interpreting aeromagnetic data. Geophysics, 35:293-302.Spector, A., Grant, F.S. (1970). Statistical models for interpreting aeromagnetic data. *Geophysics*, (35):293-302.

12. Mishra, D.C., Naidu, P.S., (1974): Two-dimensional power spectral analysis of aeromagnetic fields. Geophysical propesting, (22):345-534.

13. Ofoegbu, C.O., Onuoha, K.M. (1991): Analysis of magnetic data over the Abakaliki Anticlinorium of the Lower Benue Trough, Nigeria. Marine and Petroleum Geology, (8):174-183.

14. Chinwuko, A. I., Anakwuba, E., Onuba, L. and Nwokeabia, N. (2012): Interpretation of Aeromagnetic Anomalies over parts of the Upper Benue Trough and Southern Chad Basin, Nigeria. *Advances in Applied Science Research*, 3(3): 1757-1766.

15. Cooley, J.W., and Turkey, J.W. (1965).An algorithm for the machine calculation of complex Fourier series.*Mathematics of Computation*, (19):297-301.

16. David, I. I and Umego, M.N., (2013): Interpretation of aeromagnetic anomalies over some parts of lower Benue trough using spectral analysis technique. *International journal of scientific and technology research*. 2(8): 2277-8616.

17. Emmanuel, K.A., Ajana, G.O., Augustine, I.C. and Leonard, N.O. (2011): The interpretation of the aeromagnetic anomalies over Maiduguri-Dikwa depression, Chad Basin Nigeria. *Archives of Applied Science Research*, 3(4):499-508.

18. Hartley, R.W., and Allen, P.A., (1994): Interior cratonic Basins of Africa: Relation to continental break-up and role of mantle convection. Basin research (6):95-113.

19. Kassidy, S. and Nur, A. (2012): Analysis of Aeromagnetic data over Mutum-Biyu and its environs, Northeastern, Nigeria. *Research Journal in Engineering and Applied Sciences* 1(2):142-148.

20. Klein, G.D., and Hsui, A.T., (1987): Origin of intrcratonic Basin. Geology (15):1094-1098.

21. Lawal, T.O., and Nwankwo, L.I., (2014): Wavelet analysis of High resolution Aeromagnetic (HRAM) data over part of Chad Basin, Nigeria. *Ilorin Journal of Science*, (1)110-120.

22. Leighton. M.W., and Kolata, D.R., (1990): Selected interior cratonicBsins and their place in the scheme of a global tectonics. *American Association of petroleum Geologist memoir*. (51):729-797.

23. Mohammed, Y.B.andTela, B.M. (2012): Assessment of tertiary sediments of Bornu Basin for possible hydrocarbon reservoir. *Research Journal in Engineering and Applied Sciences*. 1(4):251-257.

24. Negi, J.G. Agrawai, P.K., Rao, K.N. (1983). Three dimensional model of the Koya area of Maharashtra state (India) based on the spectral analysis of aeromagnetic data. Geophysics, (48):964-974.

25. Nsikak, E.B., Nur, A. and Gabriel, I.D. (2000): Analysis of aerial photographic data over Guyuk area, Norhteastern Nigeria. *Journal of Mining and Geology* 36(2):145-152.

26. Nwankwo, C.N and Ekine, A.S. (2009): Geothermal gradient in the Chad Basin, Nigeria, from bottom hole temperature logs. *International Journal of physical sciences*, 4(12): 777- 783.

27. Ofoha, C.C. (2015): Structural interpretation of aeromagnetic data over parts of offshore Niger Delta, Nigeria. Msc thesis, University of Port Harcourt, Choba, Nigeria, (Unpubl) .

28. Olugbemiro, R.O., Ligouis, B., and Abaa, S.I., (1997): The Cretaceous Series in the Chad Basin, NE, Nigeria: Source rock potential and thermal maturity. Journal of Mining and geology, 20(1), 51-68.

29. Salako, K.A. (2014): Depth to basement determination using Source Parameter Imaging (SPI) of aeromagnetic data: An application to upper Benue Trough and Borno Basin, Northeastern, Nigeria. *Academic Research International*, 5(3): 54-57.

30. Schubert, G., Solomon, S.C., Turcotte, D.L., Drake, M.J., and Sleep, N.H. (1992): "Origin of Thermal Evolution of Mars". *Mars*. H.H. Kieffer, B.M. Jakonsky, C.W. Synder, and M.S Matthews (eds.). Univ. Arizona Press: Tucson, AZ. 147- 183.

31. Solomon, S.C. and Head, J.W. 1990.*J. Geophysics Res*. (95):11073-11083.

32. Squyre, S.W.,(1992): "Temperature Distribution". In: *Mars*. H.H. Kieffer, B.M. Jakonsky, C.W. Synder, and M.S Matthews (eds.). Univ. Arizona Press: Tucson, AZ. 523-554.

33. Udensi, E.E., Osazuwa, I.B.,andDaniyan, M.A. (2003). The origin and tectonic evolution of the Nupe basin, Nigeria from aeromagnetic study. Journal of Pure and Applied Sciences, 5(2):114-118.

34. Wright, J.B., Hastings, D., Jones, W.B., Williams, H.R. (1985): Geology and mineral resources of West Africa. George Allen and Urwin, London.

35. Zuber, T.M., Solomon, S.C., Phillip, R.J., Smith, D.E., Tyler, G.C., Aharonson, O, Balmino, G., Barnerdt, W.O, Head, J.W., Johnson, C.L., Lemoina, F.G., McGovern, P.G., Newmann, G.A, Rowlands, D.D., and Zlong, S.(2000): "Internal Structure and Early

Thermal Evolution of Mars: From Mars Global Surveyor Topography and Gravity". *Science*. (287)1788-1793.